Electronic Supplementary Material (ESI) for Nanoscale.

Supporting Information

Thermo- and pH-Responsive Fibrillization of Squid Suckerin A1H1 Peptide

Yunxiang Sun[1,2,*], and Feng Ding[2,*]

[1] Department of Physics, Ningbo University, Ningbo 315211, China

[2] Department of Physics and Astronomy, Clemson University, Clemson, SC 29634, United States

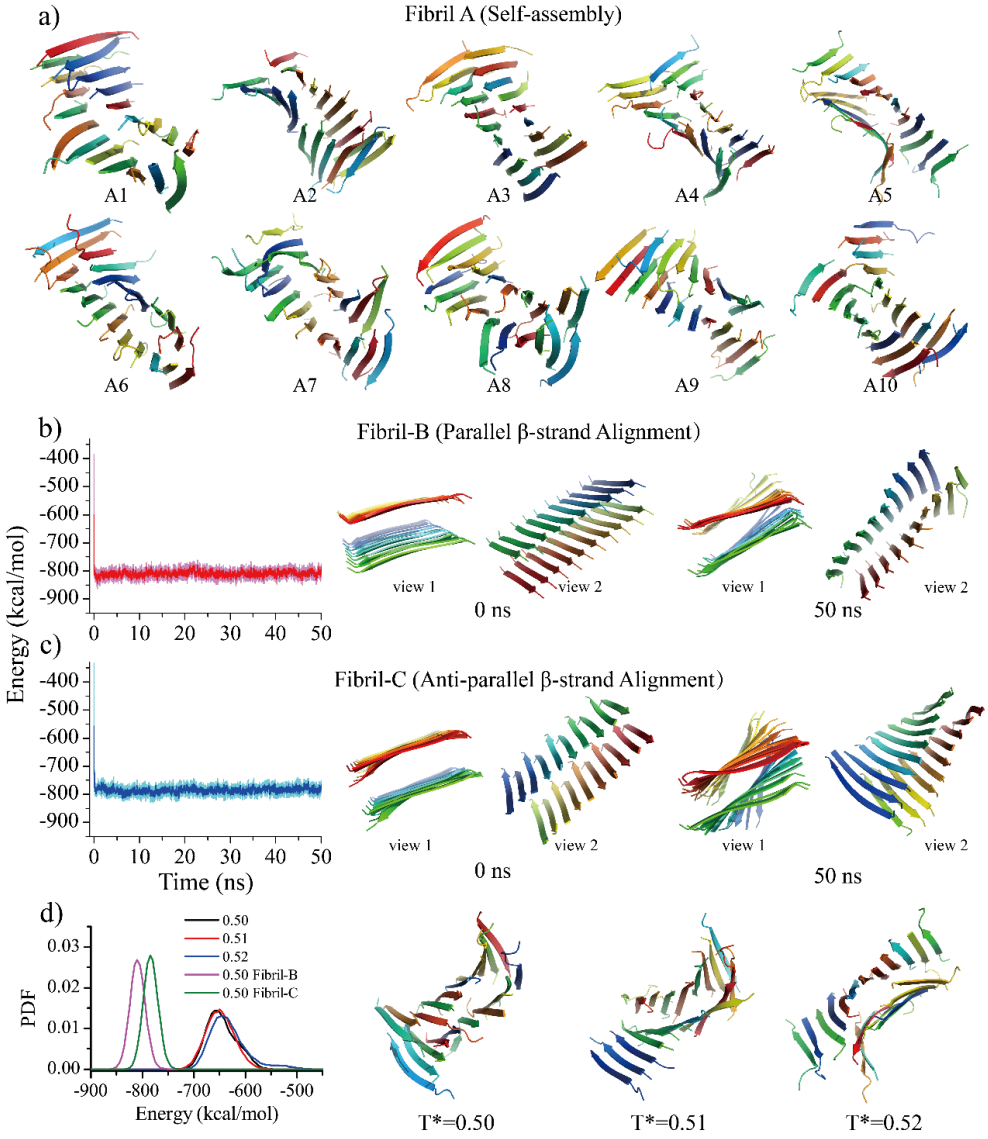

Fig. S1. **The pre-formed A1H1 fibril structures used in dissociation simulation.** a) Ten two-layer cross β-sheet fibril structures (Fibril-A) are randomly selected from the low-temperature (0.50~0.52) self-assembly DMD simulations where both parallel and anti-parallel β-sheets were observed. b-c) Ideal parallel (type-B) and anti-parallel (type-C) fibrils were also reconstructed and optimized with 50 ns low temperature simulations at T=0.50. d) Energy distribution of the three different types of A1H1 fibrils.

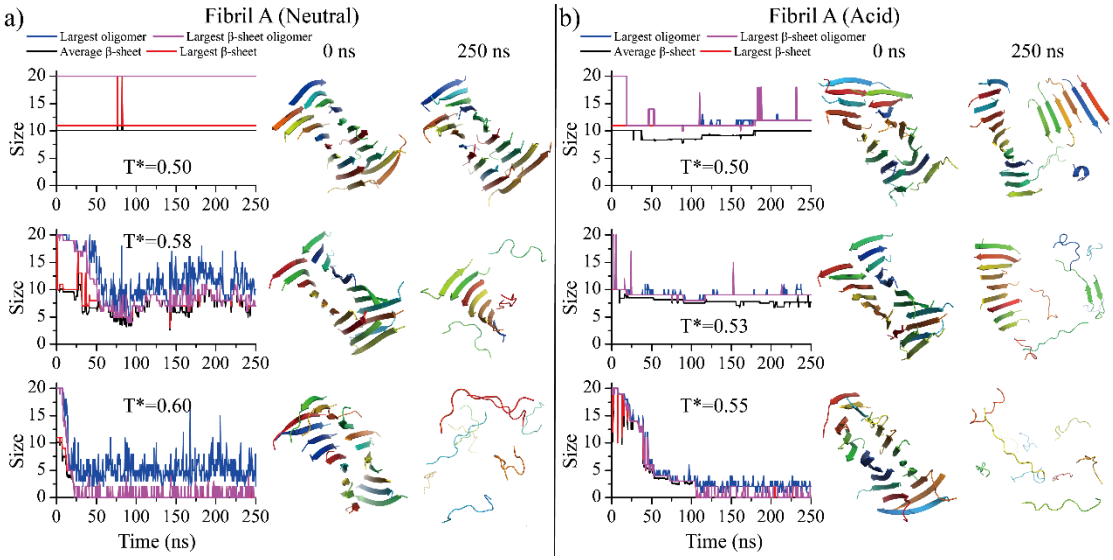

Fig. S2. **The dissociation of self-assembled fibrils.** Sizes of the largest oligomer (blue), the largest β-sheet (red), and the largest β-sheet oligomer (purple) as well as the mass-weighted average β-sheet size (black) are plotted as a function of the simulation time at different temperatures in the a) neutral and b) acidic conditions. Initial and final snapshots are shown to the right.

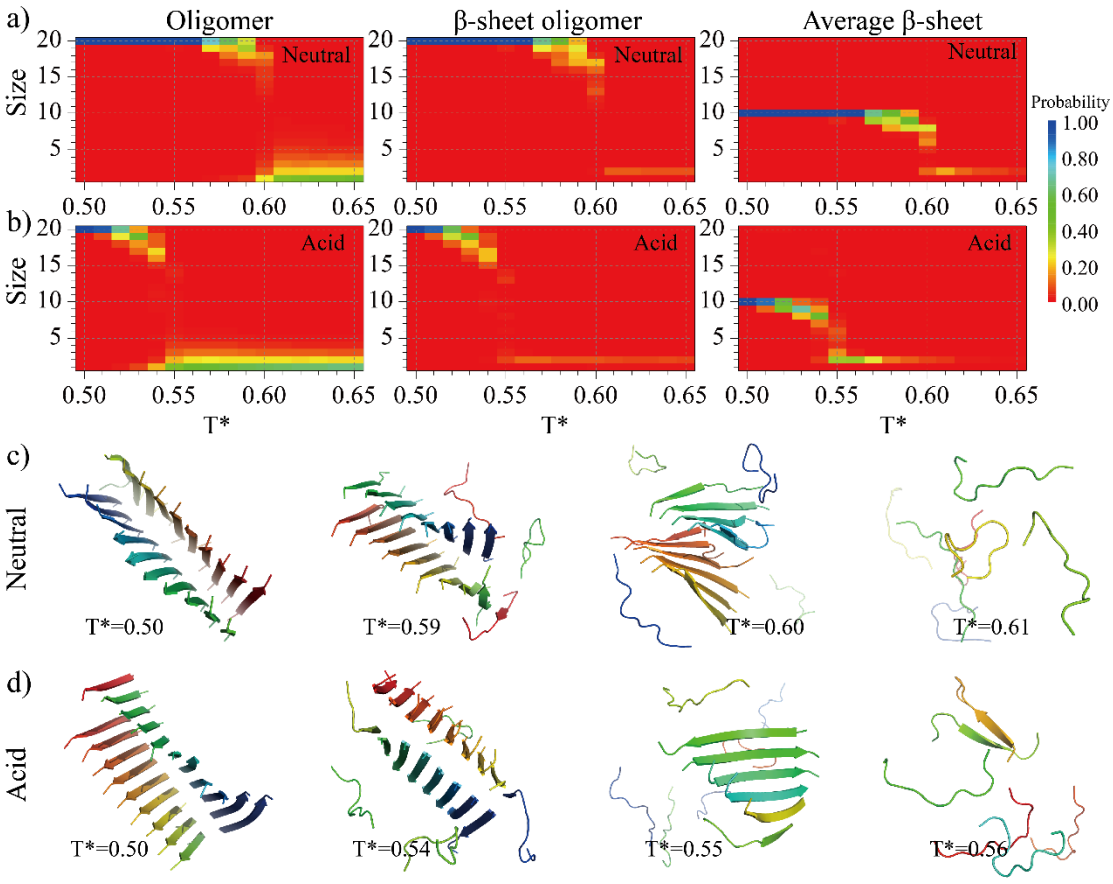

Fig. S3. **The dissociation of ideal parallel nano-fibrils at different temperatures in neural and acidic environments**. In a) neutral and b) acidic environments, the probability distributions of oligomer sizes, β-sheet oligomer sizes, and mass-weighted averaged β-sheet sizes are plotted at different temperatures for the dissociation simulations of the pre-formed anti-parallel nano-fibrils (type B in Fig. 3&S1). The last 50 ns trajectories of the 10 independent 250-ns simulations are used. Representative dissociated structures of fibril B at low, near transition and high temperatures are selected from simulations in the c) neutral and d) acidic conditions.

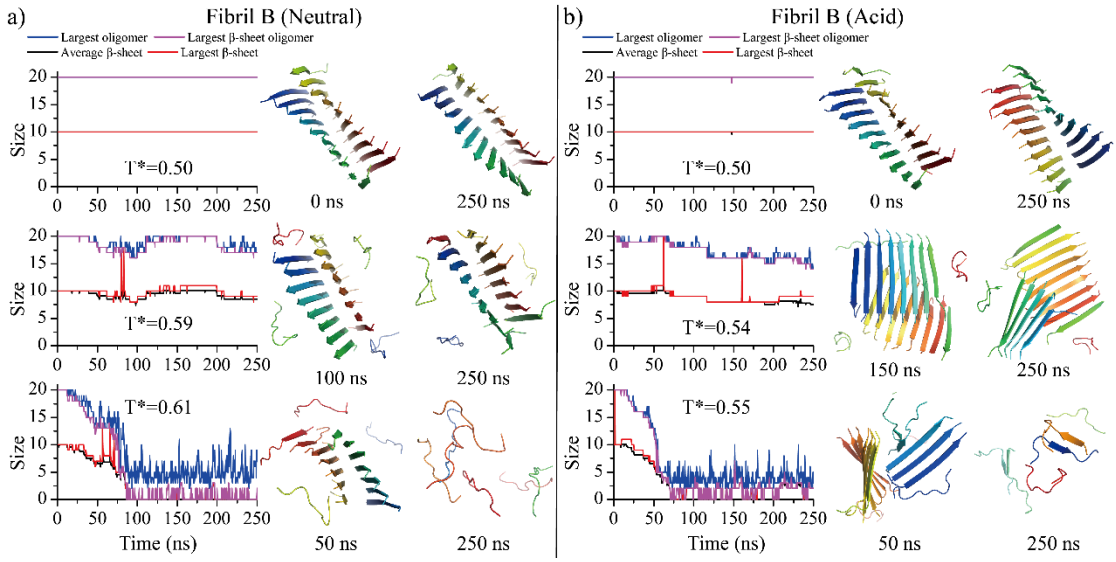

Fig. S4. **The dissociation dynamic of ideal parallel nano-fibrils.** Sizes of the largest oligomer (blue), the largest β-sheet (red), and the largest β-sheet oligomer (purple) and the mass-weighted average β-sheet size (black) are plotted as a function of the simulation time at different temperatures in the a) neutral and b) acidic conditions. Two snapshots at early and final stage are shown to the right.

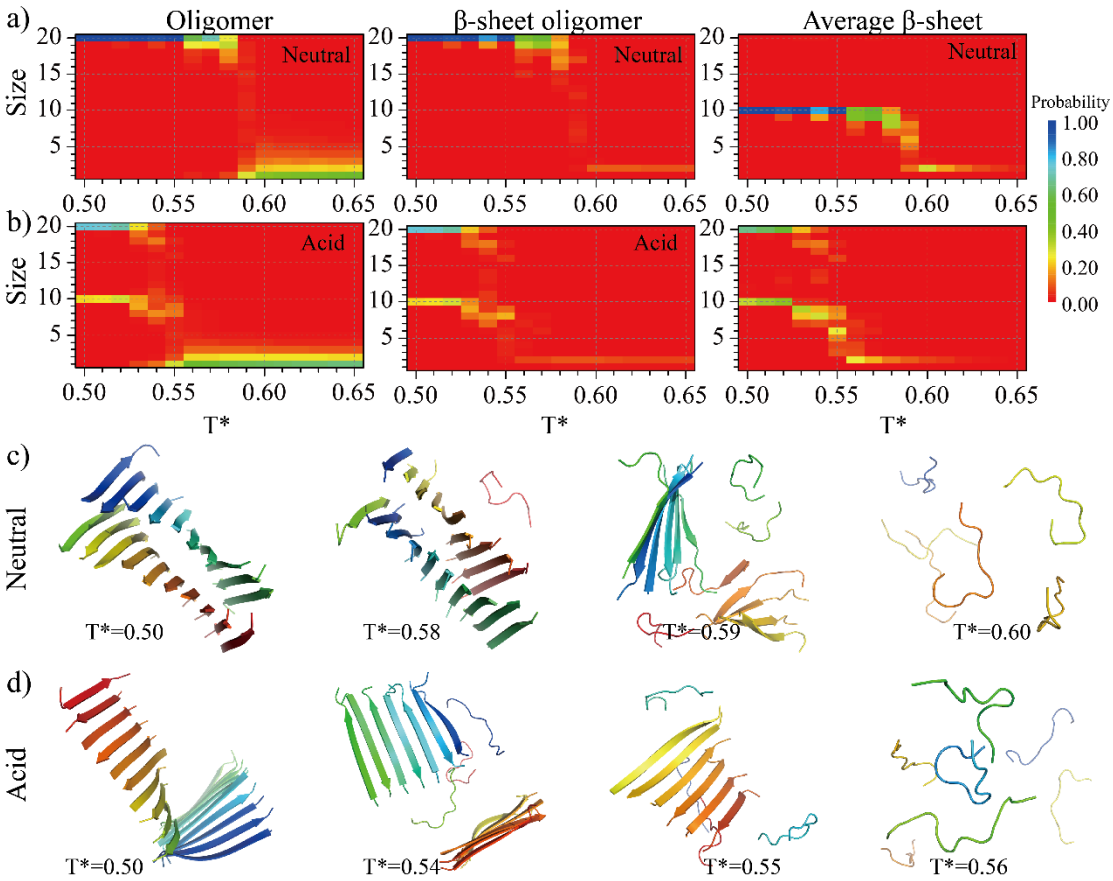

Fig. S5. **The dissociation of ideal anti-parallel nano-fibrils at different temperatures in neural and acidic environments**. In a) neutral and b) acidic environments, the probability distributions of oligomer sizes, β-sheet oligomer sizes, and mass-weighted averaged β-sheet sizes are computed at different temperatures for the dissociation simulations of the pre-formed nano-fibrils (type C in Fig. 3&S1). The last 50 ns trajectories of the 10 independent 250-ns simulations are used. Representative dissociated structures of fibril C at low, near transition and high temperatures are selected from simulations in the c) neutral and d) acidic conditions.

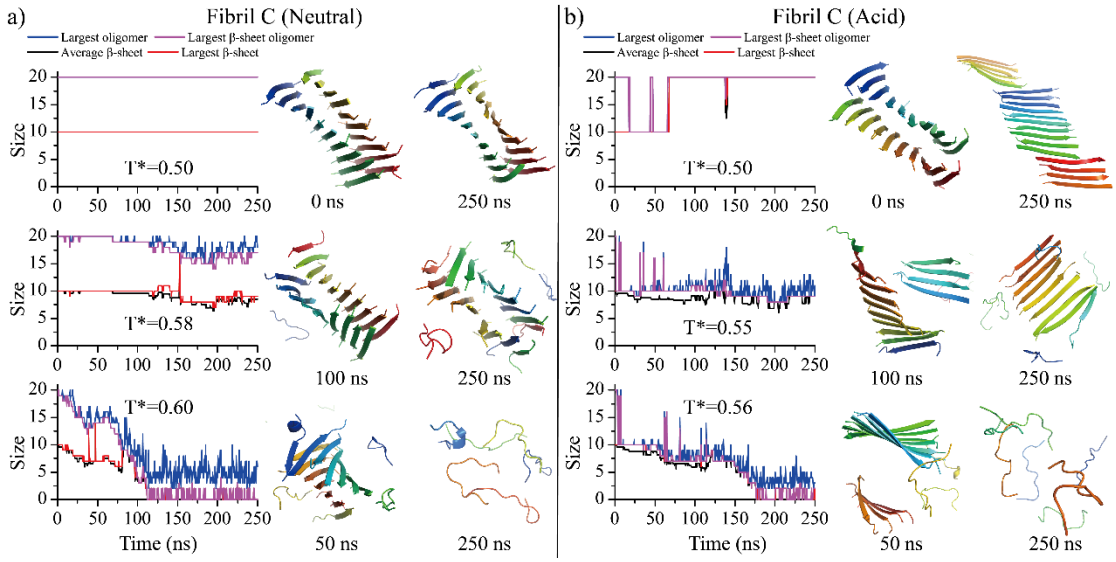

Fig. S6. **The dissociation dynamic of ideal anti-parallel nano-fibrils.** Sizes of the largest oligomer (blue), the largest β-sheet (red), and the largest β-sheet oligomer (purple) and the mass-weighted average β-sheet size (black) are plotted as a function of the simulation time at different temperatures in the a) neutral and b) acidic conditions. Two snapshots at early and final stage are shown to the right.